Phase Behavior of Ionic Clusters Down to Nanoscale. A Review of Recent Work

PEDRO C. R. RODRIGUES, FERNANDO M. S. SILVA FERNANDES

Molecular Simulation Group, CCMM, Department of Chemistry and Biochemistry, Faculty of Sciences, University of Lisboa Campo Grande, Bloco C8, 1749-016 Lisboa, Portugal

Received 16 January 2009; accepted 13 March 2009
Published online 26 May 2009 in Wiley InterScience (www.interscience.wiley.com).
DOI 10.1002/qua.22263

ABSTRACT: As finding an exact and manageable partition function for nanoclusters is a desirable but, so far, unattainable task, approximated treatments are proposed to explain and predict phase changes and phase coexistence at these size scales. In this article, a review of those approaches is presented, mainly focusing the authors work on the subject. The foundations and limitations of the proposed models are discussed and perspectives for extended treatments are given. The discussions are illustrated with new molecular dynamics simulations of unconstrained NaI and NaCl clusters. © 2009 Wiley Periodicals, Inc. Int J Quantum Chem 110: 284–292, 2010

Key words: nanoaggregates; phase change; phase equilibria; nonequilibrium phase change

1. Introduction

Phase transitions are known to be present in everyday life situations. Some of their properties are even part of common sense. For example, many people become surprised if some substance freezes at a temperature different from its melting point. This phenomenon (hysteresis) is usually associated with nonequilibrium (metastable) conditions, resulting from high cooling rates of a liquid melt and reversible paths are expected for carefully managed experiments. However, even for simple and pure substances, irreversible melting can occur, that is, cooling the melt (at any cooling rate, even with seeding) never results in a crystal [1] and more complex paths can arise. For these substances, a phase change is not completely described by concepts like, for example, the melting point. As a consequence of this complexity, a particular care should be taken to choose the convenient parameters that unambiguously characterize a system during a phase change. In this context, regardless of its constitution, a system with a finite size (for which the energy contributions either of the interfaces with the outside or of the interphases cannot be ignored) will present additional features. Such contributions prevent the system to remain at a fixed temperature during the phase conversion [2–10], often resulting in a strongly nonlinear behavior.

Correspondence to: P. C. R. Rodrigues; e-mail: reis@fc.ul.pt
Contract grant sponsor: Fundação para a Ciência e Tecnolgia (FCT, Portugal).

The main objective of the article is to review, although not exhaustively, the strategies and models proposed to deal with these behaviors, discuss their foundations, and limitations, and trace out some possible developments. In Section 2, the natural variable for phase change studies is discussed. Computational details are given in Section 3. Section 4 is devoted to the introduction of the coexistence model for clusters. In Section 5, examples of the model application to NaI and NaCl unconstrained clusters, not reported previously, are given. Section 6 contains a complementary view of the phase coexistence model foundations. Finally, some concluding remarks and perspectives of future development are given in Section 7.

2. The Natural Variable for Phase Change

Temperature, like other intensive properties, is often selected as one of the key parameters to control and characterize the state of a system. Among other reasons, this choice is related with the usual interest in studying macroscopic systems in equilibrium states, where the intensive properties tend to be homogeneous and isotropic, and to the experimental accessibility of this property in opposition to what happens, for example, with the total energy. In this context, temperature is also used to identify or characterize phase transitions. However, a carefull analysis unravels that the total energy (abbreviated to "energy" from here on) is a more convenient, or the natural variable for this specific task. In fact, it is not hard to find good reasons to look for a temperature substitute. For example, when one says that temperature remains constant during melting or freezing, at constant pressure, it is implicit that some other system properties are changing, and a single value of the temperature might not be a good choice as a parameter to follow their complete evolution.

To analyze this, consider the Figure 1(a) schematically representing the evolution of the energy as a function of the temperature for a bulk system coupled to a thermostat in the neighborhood of a first-order transition. The energy evolution is, in general, nearly linear before and after the transition temperature where it sharply changes.

Figure 1(b) corresponds to the behavior observed in the same system heated or cooled by means of successive small energy fluxes and subsequent isolation of the system after each flux (Section 2). In this case,

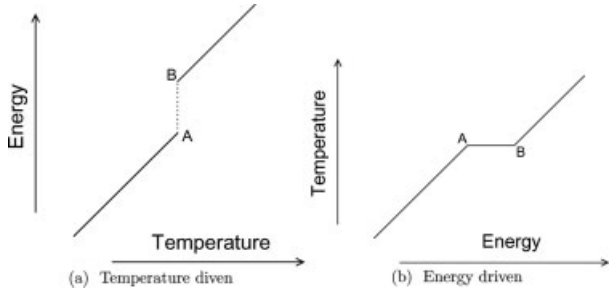

FIGURE 1. Interrelation between energy and temperature in bulk systems during a phase transition.

the temperature is left unrestrained to evolve accordingly to the structural modifications of the system and may suffer significant variations. The vertical dotted line in Figure 1(a) emphasizes that, despite $E(T)$ being not continuous from a strict mathematical point of view, the phase transformation of a real system follows that path with a finite speed determined by the thermal conductivities and heat capacities of the intervening systems.

Supposing that we are dealing with a solid–liquid transition, A [in sub-figures (a) and (b), of Fig. 1] represents the maximum energy and temperature values for which the system remains solid during the heating and, simultaneously, the temperature and energy of the system after returning completely to the solid state. Similarly, B represents the temperature and energy of the system immediately after becoming completely liquid and, simultaneously, the minimum temperature and energy for which the system remains completely liquid during the cooling.

If one does not require a complete description of all the varying properties of the system during the transformation, then the two representations and the associated procedures are totally equivalent.

Consider now Figure 2(a) where overheating and undercooling are present (the equilibrium situation is also represented as a guide to the eye). Overheating occurs when the system overcomes the equilibrium transition temperature T_A, at point A, and continues heating up till the temperature $T_{A'}$ where the transition is effectuated by a sharp energy increase since the system has reached the point of absolute instability. Similarly, overcooling occurs when the system underpasses the equilibrium transition temperature $T_B = T_A$, at the point B, and keeps cooling down until the transition takes place at temperature $T_{B'}$. Figure 2(b) contains the schematic representation of temperature evolution as a function of the energy

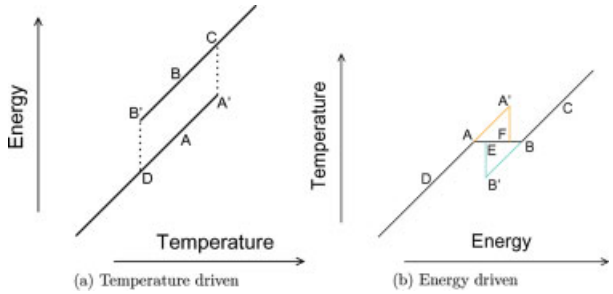

FIGURE 2. Schematic behavior of phase changes in infinite systems presenting hysteresis. [Color figure can be viewed in the online issue, which is available at www.interscience.wiley.com.]

for the same system heated, or cooled, by controlled energy fluxes.

Supposing, again, that we are in presence of a solid-liquid transition, A′ [in sub-figures (a) and (b), of Fig. 2] represents the maximum temperature and energy for which the system remains completely solid during heating. Similarly, B′ represents the minimum energy and temperature where the system remains completely liquid during cooling. However, because of the presence of overheating and undercooling, the system presents now different behaviors depending on the system being driven by temperature or energy. In the case of temperature control, the solid–liquid transition is a leap from A′ to C and the liquid–solid transition is a leap from the point B′ to the point D, for at these temperatures the absolute instability of the system has been reached as already referred to above. Therefore, phases coexistence is not sustained. In the other case, it suffices tiny energy fluxes, and subsquent isolation of the system, to its temperature decrease or increase, solely by internal structural alterations, until the phase equilibrium temperature is attained. Thus, the solid–liquid transition follows the path $A' \rightarrow F \rightarrow B$ and the liquid–solid one follows the path $B' \rightarrow E \rightarrow A$.

It should be pointed out that the diagram in Figure 2(b) contains more information than the one in Figure 2(a). For example, if the equilibrium temperature is not known at the outset, it can be accessed from 2(b) but not from 2(a).

Now, let us outline the limiting behaviors of unconstrained (virtually at zero external pressure) ionic clusters based on our simulation results. Figure 3(a) sketches the diagram for a cluster, driven by energy control, where overheating and undercooling are absent, but phases coexistence turns out along the transition region. The melting and freezing temperatures T_A and T_B, respectively, are significantly different, in contrast with the bulk situation [see Fig. 1(b)]. In fact, as we shall detail ahead, at the onset of melting the size of a cluster is always less than the critical nucleus size and phase coexistence cannot be sustained, unless the system decreases itstemperature freely until a critical nucleus is attained. Thus, the nature of controlling the energy, by small fluxes of heat and subsquent isolation (designated as a "constant or fixed energy process"), allows the system to adjust the internal kinetic and potential energies, at constant total energy: melting decreases and freezing increases the temperature. Yet, if a constant temperature, for instance T_A, is imposed upon the cluster, it is unable of sustaining phases coexistence, jumping to a higher energy at about that temperature [similar to Fig. 2(a), replacing A by A′]. Therefore, the two processes of driving the system, by constant energy or by constant temperature, are not at all equivalent: one is able to unravel phases coexistence, the other is not. From the last one, the determination of the molar fractions of the coexistent phases, and other related properties [11], is out of the question. As such, the total energy, instead the temperature, turns out as the natural variable at least for clusters.

Figure 3(b) displays the case of superheating and supercooling. The line of phase coexistence is also indicated just as a guide to the eye. This figure is analogous to Figure 2(b) for the bulk apart from the inclination of the coexistence line. The path followed, isolating the cluster after tiny fluxes of the energy, is similar to the bulk one because of the reasons given earlier.

As we shall see in the examples ahead, deviations from the foregoing limiting situations are generally observed, depending essentially on the number of ions, n, in the clusters. Yet, when $n \rightarrow \infty$ the clusters approach the bulk behavior as expected. This is one

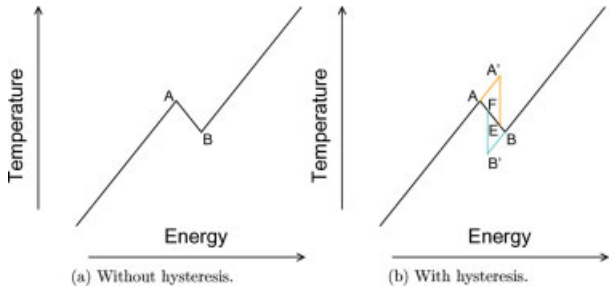

FIGURE 3. Schematic behavior of phase changes in finite systems driven by energy. [Color figure can be viewed in the online issue, which is available at www.interscience.wiley.com.]

of our starting points for the theoretical model in Section 4.

3. Computational Details

In molecular dynamics simulations, heating or cooling a system under controlled energy fluxes is achieved by rescaling the velocities using a factor (slightly greater or less than 1, respectively), subsquently isolating the system, calculating its properties after a complete relaxation, and then making the next rescaling.

The coupling to a thermostat is obtained by any suitable constant temperature method, such as damped-force or Nosé–Hoover techniques [12, 13] to fix, or drive the system, to the desired temperature. In this case, a phase change is induced by smoothly increasing or decreasing the temperature in small steps along the phase change region. All those techniques produce equivalent results outside the phase transition regions. However, as discussed in the previous section, this is not the case inside those regions. Moreover, the damped-force method, for example, frequently gives rise to nonphysical behaviors (instantaneous transitions) or numerical instabilities on phase transition simulations.

Most of the molecular dynamics computations have been performed using the Born–Mayer–Huggins (BMH) potential:

$$\phi_{ij}(r) = \frac{z_i z_j e^2}{r} + c_{ij} b \exp\left[\frac{\sigma_{ij} - r}{d}\right] - \frac{C_{ij}}{r^6} - \frac{D_{ij}}{r^8} \quad (1)$$

with the parameters given by Watts and McGee [14].

However, to analyze the relative stability of the clusters at 0 K, we have also done some calculations [15] with the Michielsen–Woerlee–Graaf (MWG) potential:

$$\phi_{ij}(r) = \frac{z_i z_j e^2}{r} + \frac{b}{r^l} \exp\left[k_{ij}\left(\sigma_{ij}^m - r^m\right)\right] - \frac{C_{ij}}{r^6} - \frac{D_{ij}}{r^8} \quad (2)$$

with the parameters given by Michielsen et al. [16] for $l = 4$ and $m = 1$. It is well known that these interaction models, despite being rigid-ion potentials, reproduce some bulk properties of alkali halides and other substances [17–23]. Recently, we have reported [24] an extensive study, by molecular dynamics and free energy calculations, of the phase diagrams for bulk KCl and NaCl, using those models.

Verlet's leapfrog algorithm [12] for the numerical integration of Newton's equations of motion, with a time step of 5×10^{-15} s, has been used in all simulations. Thermal properties have been calculated with a number of steps in the range $10^5 - 10^8$, depending on the size of the clusters and the phase transition region. Thus, the longer runs correspond to time scales of the order of 10^2 ns.

4. Phase Coexistence Model

An exact and complete treatment of phase transitions and coexistence of a system requires the respective partition function [25, 26]. This is a challenging task, even for the simplest systems [27, 28], and restrictive approximations are unavoidable for the more complex ones [29]. The partition function approach has, however, been used for very small systems that are not able to sustain phase coexistence [29, 30].

Such small systems either dynamically oscillate between ordered and disordered conformations [29] (observed up to ~100 ions for alkali-halides clusters [31]) or present sharp jumps between ordered and disordered phases, with hysteresis cycles when heated and cooled (observed from ~100 up to ~1000 ions also for alkali-halides clusters [31]). Bigger systems presenting sustained phase coexistence (for example, in the form of two regions: one solid-like and the other liquid-like separated by a permanent interface), as observed for alkali-halides clusters, with sizes over 1,000 ions, require a different approach. By making geometric restrictions to the shapes of the component phases, it is possible obtain a relation between the system variables [32]. A less restrictive model in what concerns solid and, specially, liquid shapes, proposed by the authors [11], is discussed in the following.

The model construction, focusing solid–liquid transitions, uses the bulk behavior as a reference and introduces corrections to account for finite size effects. In a bulk system, after the melting onset and solid–liquid equilibrium is attained, adding energy to the system converts a portion of solid to liquid, with the temperature and pressure remaining constant. The number of particles in the solid phase, at a given energy E, is:

$$n_s^{\infty} = \frac{E_{l(T_m)} - E}{E_{l(T_m)} - E_{s(T_m)}} n \quad (3)$$

where $E_{s(T_m)}$ and $E_{l(T_m)}$ are, respectively, the total energy of the bulk solid and liquid at the melting

temperature T_m, and n is the total number of paricles in the system.

In a finite system (cluster), a crystallite with size n_s, vitually produced at any given energy over the bulk solid–liquid line, will be smaller than the critical nucleus, n^*, which, accordingly to classical nucleation theory [11, 33, 34], is given, as a function of the temperature, T, by

$$n^* = k^3 \frac{T_m^3}{(T_m - T)^3} \tag{4}$$

for any nuclei geometry. The function k is defined ahead. This equation pressuposes, in its derivation, a bulk liquid phase, which it is not strictly true for clusters. Nonetheless, we have observed that for a considerable number of cases, this relation is still a good approximation down to nanosized clusters with ~1,000 particles, either at fixed temperature or energy [35] and we assume it in a first approach.

Because the size of the critical nucleus, at the melting temperature, T_m, approaches infinity, the crystallite at that temperature shall shrink and disappear. As the presence of, at least, a solid embryo, large enough to overcome the free energy barrier, is required to achieve a sustained solid–liquid coexistence (the dynamics of this is discussed ahead in the Section 6), a number of particles in the solid, Δn_s, shall be transferred to the liquid until a critical nucleus is formed. However, because the total energy is fixed during that transference a variation in the phases composition implies a simultaneous temperature decrease, $\Delta T = T - T_m$, resulting from the conversion between kinetic and potential energies [11], approximately expressed as:

$$\Delta T = \frac{\Delta n_s \Delta h}{n C_p} \tag{5}$$

where Δh and C_p are, respectively, the enthalpy of melting and the heat capacity.

The number of solid particles in the cluster is

$$n_s = n_s^{bb} + \Delta n_s \tag{6}$$

where n_s^{bb}, given by the same form of Eq. (3), should be understood as the number of solid particles that the cluster should have if it followed the bulk behavior. $E_{s(T_m)}$ and $E_{l(T_m)}$ of Eq. (3) are now the projected solid and liquid cluster energies at the bulk melting temperature, T_m. Combining the two last equations with Eq. (3), the size of the crystallite as a function of energy and temperature is:

$$n_s = \frac{E_{l(T_m)} - E}{\Delta h} n + \frac{(T - T_m) n C_p}{\Delta h} \tag{7}$$

Phase coexistence is attained when the crystallite size, given by the last equation, becomes equal to the size of the critical nucleus, maximizing the entropy of the system [36, 37] (Section 6). Therefore, after straightforward algebric manipulations, the key equation of the phase coexistence model [11] is then:

$$E = E_{l(T_m)} + (T - T_m) C_p - k^3 \frac{\Delta h T_m^3}{n (T_m - T)^3} \tag{8}$$

This equation allows the prediction of the (T, E) curves for direct comparision with experimental or simulation results.

Apart from the foregoing referred to approximations, the presented equations can be applied to any kind of clusters. However, some definitions are still needed [11, 35]. In the previous equations, k (for the specific case of cubic nucleus, the ones of interest for alkali halides) is given by:

$$k = \frac{4 \upsilon^{\frac{2}{3}} \sigma}{\Delta h} \tag{9}$$

where υ is the specific volume of the solid, σ is the surface tension of the solid–liquid interface, and

$$E_{l(T_m)} = E_{l(T_m)}^{\infty} + \varsigma_l n^{-\frac{1}{3}} \tag{10}$$

$E_{l(T_m)}$ is the total energy of the cluster at, or projected to, the bulk melting temperature, T_m. $E_{l(T_m)}^{\infty}$ is the respective bulk limit energy, ς_l is the rate of change of the cluster total energy with system size, n, and

$$\Delta h = \Delta h^{\infty} + \Delta \varsigma n^{-\frac{1}{3}} \tag{11}$$

Δh is the cluster enthalpy of melting, Δh^{∞} is the respective bulk limit, $\Delta \varsigma$ is the rate of change of the melting enthalpy with system size, and C_p is the average of the heat capacities for the solid and liquid bulks taken near the melting point. Solid–vapor and liquid–vapor interfacial energies are implicitly considered in Eq. (11) for the variation of the melting enthalpy with system size.

From the model, several properties can be predicted as, for example, the cluster melting start and end points, respectively,

$$T_{if} = T_m \left(1 - k n^{-\frac{1}{3}}\right) \tag{12}$$

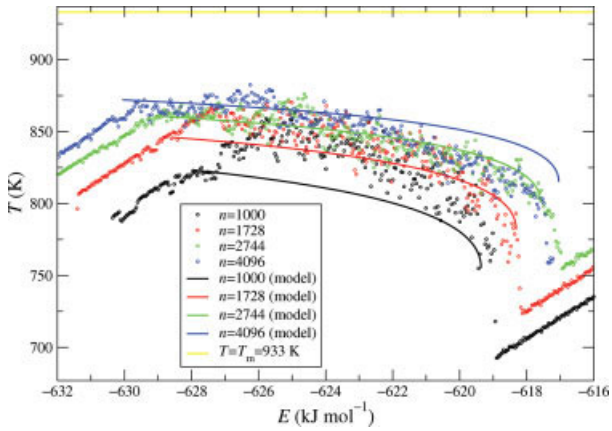

FIGURE 4. Phase coexistence model prediction versus simulation results for a set of NaI clusters. [Color figure can be viewed in the online issue, which is available at www.interscience.wiley.com.]

and

$$T_{\text{inf}} = T_{\text{m}} - \left(\frac{3k^3 T_{\text{m}}^3 \Delta h}{nC_{\text{p}}}\right)^{\frac{1}{4}} \tag{13}$$

as well as the corresponding energies E_{if} and E_{inf} [11]. These properties are particularly interesting regarding the discussions ahead for which it is important to note that the model predicts starting melting temperatures less than the ones for the bulk. Thus, we have designated the melting of the clusters in the interval $[T_{\text{if}}, T_{\text{m}}]$ by "early melting."

The model also predicts other properties accessible from simulations, some of them even from experiment [38]. They have been recently reported elsewhere [11, 15].

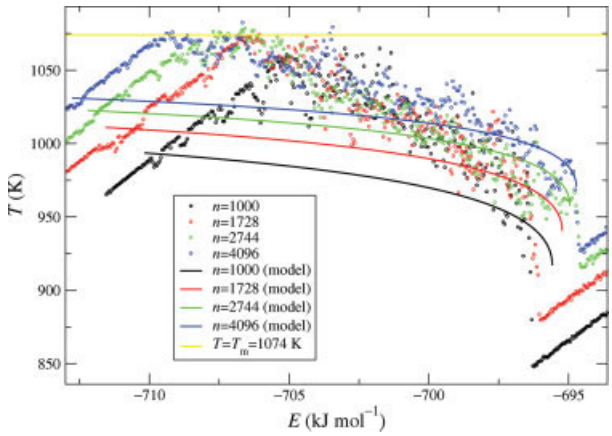

FIGURE 5. Phase coexistence model prediction versus simulation results for a set of NaCl clusters. [Color figure can be viewed in the online issue, which is available at www.interscience.wiley.com.]

TABLE I

Enthalpy of melting, in kJ mol^{-1}, and heat capacity, in J K^{-1} mol^{-1}, of solid and liquid NaI clusters at the bulk melting temperature $T_{\text{m}} = 933$ K.

n	$C_{\text{p}}^{(\text{s})}$	$C_{\text{p}}^{(\text{l})}$	Δh
1,000	75.19	69.58	17.53
1,728	68.01	70.53	19.37
2,744	68.27	68.96	19.52
4,096			
∞			
exp	59.95	64.85	23.60

5. Examples of the Model Application to NaI and NaCl Clusters

Figures 4 and 5, and Tables I and II contain, respectively, new results [39] for molecular dynamics simulations of NaI and NaCl clusters with sizes between 1,000 and 4,096 ions. Despite noticeable differences relatively to KCl [31, 35] and LiCl [15] clusters, these results follow the main trends of the alkali halides melting behavior.

The results in Figure 4 for the NaI clusters were obtained by using the parameters: $T_{\text{m}} = 933$ K, $k^{\infty} = 0.88$, $C_{\text{p}} = 69\,\text{J K}^{-1}\,\text{mol}^{-1}$, $E^{\infty}_{\text{l}(T_{\text{m}})} = -611.5\,\text{kJ mol}^{-1}$, $\varsigma_{\text{l}} = 84.906\,\text{kJ mol}^{-1}$, $\Delta h^{\infty} = 23.6\,\text{kJ mol}^{-1}$, $\Delta\varsigma = -58\,\text{kJ mol}^{-1}$. As expected, taking into consideration that the model assumes a bulk liquid phase (and the equations are considered only approximately valid with a finite liquid phase as referred to in Section 4), the predictions are more accurate for larger clusters, and the more significant deviations, if any, tend to occur at the initial stages of the melting when the most part of the cluster is solid and the liquid part is just a small drop on a side or a thin layer on one or two faces. The model prediction divergence from

TABLE II

Enthalpy of melting, in kJ mol^{-1}, and heat capacity, in J K^{-1} mol^{-1}, of NaCl solid and liquid clusters at the bulk melting temperature $T_{\text{m}} = 1,074$ K.

n	$C_{\text{p}}^{(\text{s})}$	$C_{\text{p}}^{(\text{l})}$	Δh
1,000	69.03	70.57	23.80
1,728	67.44	70.67	24.38
2,744	66.90	70.70	24.97
4,096	66.74	69.70	25.25
∞			27.75
exp	67.36	70.37	28.25

the simulation results for the 4,096 ions cluster, over $-622\,\mathrm{kJ\,mol^{-1}}$, is an exception to the general trend. This singular behavior is suspected to be due to a change from a partial wetting to a total immersion of the crystallite in the melt and requires a further investigation. The main conclusions are, therefore: (i) excluding the 4,096 ions case, the melting end temperatures are correctly predicted; (ii) the melting start temperatures of the bigger clusters (2,744 and 4,096 ions) are in good agreement with simulations; (iii) the melting start temperatures of the smaller clusters (1,000 and 1,728 ions) are a bit underestimated; and (iv) early melting is observed according to the model predictions similarly to what has been reported for LiCl clusters [15].

The results in Figure 5 for the NaCl clusters were obtained with the parameters $T_\mathrm{m} = 1{,}085\,\mathrm{K}$, $k^\infty = 0.72$, $C_\mathrm{p} = 68\,\mathrm{J\,K^{-1}\,mol^{-1}}$, $E^\infty_{\mathrm{l}(T_\mathrm{m})} = -690.98\,\mathrm{kJ\,mol^{-1}}$, $\varsigma_\mathrm{l} = 106.16\,\mathrm{kJ\,mol^{-1}}$, $\Delta h^\infty = 27.74\,\mathrm{kJ\,mol^{-1}}$, $\Delta\varsigma = -39.647\,\mathrm{kJ\,mol^{-1}}$. In this case, the simulations indicate that all the clusters closely approach the bulk melting temperature. However, the model predictions remarkably underestimate the melting temperatures, giving values well inside the solid branches. This means that the simulations do not show up early melting, similarly to what has been reported for KCl clusters [11]. Nonetheless, the end parts of the coexistence curves are correctly predicted, remaining within the fluctuations observed for all the clusters.

Thus, the NaCl case constitutes a significantly less successful application of the model mainly as far as early melting is concerned. As the model failures are undoubtedly related to the approximations discussed earlier, to trace perspectives that may aid in overcoming those limitations, a closer review of the model foundations follows in the next section.

6. Model Foundations

The minimum (reversible) work [33] to create an embryo inside a bulk liquid phase at a fixed temperature, T, and pressure, p, is:

$$W_\mathrm{min}(T,p) = \sigma(T,p)F + n_\mathrm{e}\Delta\mu(T,p) \qquad (14)$$

where n_e is the number of particles in the embryo, F is the surface area of the embryo (proportional to $n_e^{2/3}$), $\sigma(T,p)$ is the interfacial solid–liquid surface tension, and $\Delta\mu(T,p)$ is the difference between the chemical potentials of the solid and liquid phases. Equation (14) has a maximum when n_e is equal to the critical nucleus size n^* [given by Eq. (4)]. Embryos containing less than n^* particles shrink spontaneously, whereas embryos larger than n^* grow spontaneously. As such, for the formation of the new phase, the system must first overcome a free energy barrier by creating a critical nucleus.

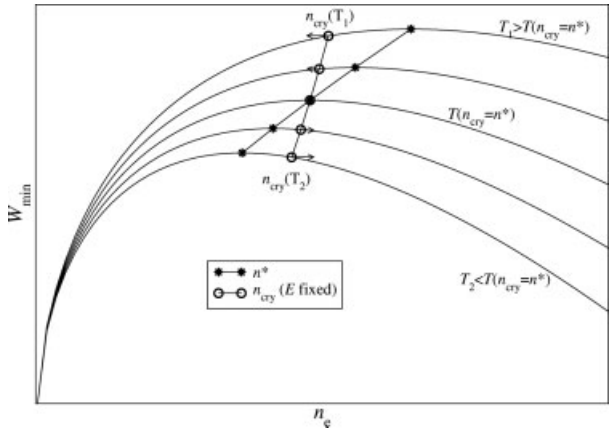

FIGURE 6. Dynamics through which a cluster attains a sustained solid–liquid coexistence at constant energy.

The coexistence model assumes, in a first approximation, that the last equation remains valid for small clusters. Figure 6 captures, qualitatively, the essential dynamics through which a cluster can sustain a solid–liquid coexistence, at constant energy and external pressure. Suppose, for example, a solid crystallite of size $n_\mathrm{cry}(T_1)$ at temperature T_1. Once its size is less than the one of the critical nucleus , $n^*(T_1)$, the cluster spontaneously melts and the crystallite shrinks. As the total energy is fixed, the temperature shall decrease until the crystallite size reaches the value $n^*(T)$, which also constitutes a critical nucleus, but now over a different work function surface. For a size less than $n^*(T)$, for example at $T_2 < T$, the crystallite would spontaneously grow (with a temperature increase at constant total energy), since such size is greater than the critical nucleus of the corresponding work function. Therefore, at $n^*(T)$ the cluster should be able to sustain solid–liquid coexistence where the entropy and free energy, in the constant energy process have, respectively, a maximum and a saddle point [36, 37].

7. Perspectives on Model Extensions

In the presented model, the slope of the work function dependence on the embryo size, $\mu = \Delta W/\Delta n_\mathrm{e}$ that indicates the height of the free energy

barrier, is evaluated supposing a bulk liquid phase, which constitutes a first approximation since clusters are finite systems. Therefore, additional constraints that can determine the states of the clusters should be considered regarding an extension of the model.

A partially melted finite system can be seen, depending on the proportions of the solid and liquid portions, either as a crystallite embryo in the presence of an unstable liquid or as a droplet embryo in the presence of an unstable solid. As such, choosing the solid portion as parameter, we can define the family of functions $W_{\mathrm{liq}}(n-n_{\mathrm{s}}, T, p)$ that may present considerable free energy barriers to droplets formation, for $T < T_{\mathrm{m}}$, like the ones presented by the family $W_{\mathrm{sol}}(n_{\mathrm{s}}, T, p)$ to crystallites formation for $T > T_{\mathrm{m}}$. The respective slopes are μ_{liq} and μ_{sol}.

In this context, the following qualitative outline can be done, based on the behaviors observed in some of our simulations and the present model predictions:

1. $\mu_{\mathrm{liq}} < \mu_{\mathrm{sol}}$ and a droplet is easily formed even at temperatures significantly lower than T_{m}. Early melting is present and the phase coexistence extends from E_{if} to E_{inf} accordingly to the model (observed in LiCl and NaI clusters).
2. $\mu_{\mathrm{liq}} < \mu_{\mathrm{sol}}$ up to the neighborhood of the bulk melting temperature, T_{m}, even for very small droplets. Nearly T_{m} the droplet formation barrier is overpassed and from there on the phase coexistence is in accordance with the model. (observed in KCl clusters).
3. $\mu_{\mathrm{liq}} < \mu_{\mathrm{sol}}$ even at the neighborhood of the bulk melting temperature, T_{m}. The system slightly overcomes T_{m} and starts melting in a overheated state until the droplet contribution becomes less significant and allows the proper crystallite contribution being attained by a fluctuation. Then, this is followed by a relatively sharp transition to the model predictions (observed in NaBr and NaCl clusters).

These outlined situations are not exhaustive Moreover, the forementioned behaviors can be simultaneously observed in the same clusters family when different sizes are considered. For example, the results for NaI clusters, in Figure 4, show that for sizes of 1,000 and 1,728 ions, despite they never come close to the bulk melting temperature, do not present a strict early melting, whereas the sizes of 2,744 and 4,096 ions do. This means that the balance between the weights of the contributions from the crystallite and the droplet changes with size. Thus, a model extension clearly needs to include, at least, the quantitative contribution of the droplet work of formation, the surface of the system (particulary for small aggregates), and the determination of the accessible coexistent states considering, at each energy value, the complete system geometry, in the spirit of the work by Cleveland et al. [32]. However, this is not easy to accomplish because of the multiplicity of geometries that can be involved, and it is the challenge of the work in progress.

ACKNOWLEDGMENTS

The authors thank the GNU and Linux communities for all of the invaluable tools they offer.

References

1. Moura-Ramos, J. J.; Correia, N. T. Phys J Chem Phys 2001, 3, 5575.
2. Kaelberer, J. B.; Etters, R. D. J Chem Phys 1977, 66, 3233.
3. Quirke, N.; Sheng, P. Chem Phys Lett 1984, 110, 63.
4. Thompson, S. M.; Gubbins, K. E.; Walton, J. P. R. B.; Chantry, R. A. R.; Rowlinson, J. S. J Chem Phys 1984, 81, 530.
5. Sakamoto, Y. J Phys Soc Jpn 1990, 59, 3925.
6. Rose, J. P.; Berry, R. S. J Chem Phys 1992, 96, 517.
7. Rose, J. P.; Berry, R. S. J Chem Phys 1993, 98, 3246.
8. Rose, J. P.; Berry, R. S. J Chem Phys 1993, 98, 3262.
9. Fernandes, F. M. S. S.; Neves, L. A. T. P. Am Inst Phys Conf Proc 1995, 330, 313.
10. Deng, H.; Huang, J. J Solid State Chem 2001, 159, 10.
11. Rodrigues, P. C. R.; Fernandes, F. M. S. S. Eur Phys J D 2007, 41, 113.
12. Allen, M. P.; Tildesley, D. J. Computer Simulation of Liquids; Claredon Press: Oxford, 1987.
13. Frenkel, D.; Smit, B. Understanding Molecular Simulation. From Algorithms to Applications, 2nd ed.; Academic Press: San Diego, 2002.
14. Watts, R. O.; McGee, I. J. Liquid State Chemical Physics; Wiley: New York, 1976.
15. Rodrigues, P. C. R.; Fernandes, F. M. S. S. Eur Phys J D 2007, 44, 109.
16. Michielsen, J.; Woerlee, P.; Graaf, F. V. D.; Ketelaar, J. A. A. J Chem Soc Faraday Trans II 1975, 71, 1730.
17. Woodcock, L. V. Chem Phys Lett 1970, 10, 257.
18. Woodcock, L. V.; Singer, K. Trans Faraday Soc 1971, 67, 12.
19. Sangster, M. J. L.; Dixon, M. Adv Phys 1976, 25, 247.
20. Cruz, F. J. A. L.; Lopes, J. N. C; Calado, J. C. G.; da Piedade, M. E. M. J Phys Chem B 2005, 109, 24473.
21. Cruz, F. J. A. L.; Lopes, J. N. C.; Calado, J. C. G. J Phys Chem B 2006, 110, 4387.
22. Galamba, N.; de Castro, C. A. N.; Ely, J. F. J Phys Chem B 2004, 108, 3658.

23. Galamba, N.; de Castro, C. A. N.; Ely, J. F. J Chem Phys 2004, 120, 8676.
24. Rodrigues, P. C. R.; Fernandes, F. M. S. S. J Chem Phys 2007, 126, 024503.
25. Ruelle, D. Statistical Mechanics. Rigorous Results; Benjamin: New York, 1969.
26. Huang, K. Statistical Mechanics; Wiley: New York, 1987.
27. Onsager, L. Phys Rev 1944, 65, 117.
28. Ferdinand, A. E.; Fisher, M. E. Phys Rev 1969, 185, 832.
29. Adams, J. E.; Stratt, R. M. J Chem Phys 1990, 93, 1332.
30. Berry, R. S.; Smirnov, B. M. J Chem Phys 2001, 114, 6816.
31. Rodrigues, P. C. R.; Fernandes, F. M. S. S. Int J Quantum Chem 2001, 84, 169.
32. Cleveland, C. L.; Landman, U.; Luedtke, W. D. J Phys Chem 1994, 98, 6272.
33. Debenedetti, P. G. Metastable Liquids, Concepts and Principles; Princeton University Press: New Jersey, 1996.
34. Markov, I. V. Crystal Growth for Beginners, 3rd ed.; World Scientific Publishing: Singapore, 1998.
35. Rodrigues, P. C. R.; Fernandes, F. M. S. S. Eur Phys J D 2006, 40, 115.
36. Nielsen, O. H.; Sethna, J. P.; Stoltze, P.; Jacobsen, K. W.; Norskov, J. K. Eur Phys Lett 1994, 26, 557.
37. Antoni, M.; Ruffo, S.; Torcini, A. Phys Rev E 2002, 66.
38. Chushak, Y. G.; Bartell, L. S. J Phys Chem B 2001, 105, 11605.
39. Rodrigues, P. C. R. Transições de Fase em Sistemas Iónicos, Modelos Teóricos e Simulação Computacional, Ph.D. Thesis, Faculdade de Ciências, Universidade de Lisboa, 2006.